

EXPERIMENTAL DETERMINATION OF THE PION AND NUCLEON STRUCTURE FUNCTIONS  
BY MEASURING HIGH-MASS MUON PAIRS PRODUCED BY PIONS OF 200 AND 280 GeV/c  
ON A PLATINUM TARGET

C.E.N., Saclay<sup>1</sup>-CERN<sup>2</sup>-Collège de France, Paris<sup>3</sup>-Ecole Polytechnique, Palaiseau<sup>4</sup>-  
Laboratoire de l'Accélérateur Linéaire, Orsay<sup>5</sup>

J. Badier<sup>4</sup>, J. Boucrot<sup>5</sup>, G. Burgun<sup>1</sup>, O. Callot<sup>5</sup>, Ph. Charpentier<sup>1</sup>, M. Crozon<sup>3</sup>,  
D. Decamp<sup>2</sup>, P. Delpierre<sup>3</sup>, A. Diop<sup>3</sup>, R. Dubé<sup>5</sup>, B. Gandois<sup>1</sup>, R. Hagelberg<sup>2</sup>,  
M. Hansroul<sup>2</sup>, W. Kienzle<sup>2</sup>, A. Lafontaine<sup>1</sup>, P. Le Dû<sup>1</sup>, J. Lefrançois<sup>5</sup>, Th. Leray<sup>3</sup>,  
G. Matthiae<sup>2</sup>, A. Michelini<sup>2</sup>, Ph. Miné<sup>4</sup>, H. Nguyen Ngoc<sup>5</sup>, O. Runolfsson<sup>2</sup>,  
P. Siegrist<sup>1</sup>, J. Timmermans<sup>2</sup>, J. Valentin<sup>3</sup>, R. Vanderhagen<sup>4</sup>, S. Weisz<sup>4</sup>

ABSTRACT

We measured the production of massive muon pairs on a platinum target by pions of 200 and 280 GeV/c. The following number of dimuon events have been collected for  $M > 4$  GeV/c<sup>2</sup>. (a)  $\pi^-$  of 200 GeV/c:  $\sim 5900$  events; (b)  $\pi^+$  of 200 GeV/c:  $\sim 2200$  events; (c)  $\pi^-$  of 280 GeV/c:  $\sim 5700$  events. These data were analysed in terms of the Drell-Yan model in order to obtain the pion and nucleon structure functions, which are parametrised with expressions of the form  $x^\alpha(1-x)^\beta$ . Our results are compared to the structure functions obtained in other experiments.

1. INTRODUCTION

We have performed a series of experiments to measure the production of massive muon pairs in hadron-hadron collisions at the CERN SPS. One of the aims of the experiment was to obtain the structure functions of unstable hadrons like pions and kaons, difficult to probe by lepton scattering, by making use of the Drell-Yan mechanism of quark annihilation.

In this paper we present detailed results on the pion and nucleon structure functions. Data on dimuon production by kaons, protons and anti-protons are discussed in another contribution<sup>1)</sup> to this conference.

2. THE EXPERIMENTAL APPARATUS

The general layout of the experiment is shown in fig. 1(a). The beam is an unseparated secondary particle beam produced by protons of 400 GeV/c on a 50 cm Be target. Particle identification is done by two differential Čerenkov counters (CEDAR's) for  $K^\pm$  and  $\bar{p}$ , and two threshold Čerenkov counters for  $\pi^+$ . The particle fluxes were in the range  $(1 - 3) 10^7$  part/pulse. At 200 GeV/c the fraction of  $\pi^-$  in the negative beam was about 96%. A 2m long CH<sub>2</sub> absorber was used to enhance the  $\pi^+$  percentage of the positive beam to about 36%.

Platinum targets, 6 cm long for the 200 GeV run and 11.1 cm for the 280 GeV run, were used. At 200 GeV we have also used a 30 cm long liquid hydrogen target.

After passing through the targets, the beam is absorbed in a beam dump which starts 40 cm downstream of the Pt target. It consists of a 1.5 m long block of stainless steel with a heavy (tungsten and uranium) conical plug of  $\pm 30$  m rad aperture inserted in the centre, in order to minimize the total beam dump length.

The large acceptance magnetic spectrometer consists of:

- i) a large superconducting dipole magnet with vertical field ( $\int B dl = 4.0$  Tm) in an airgap of cylindrical shape of 1.6 m diameter;
- ii) a set of six multiwire proportional chambers (31 planes with a total of about 26 000 wires) ranging in size from  $0.6 \times 0.6$  m<sup>2</sup> (PC1) up to  $4.2 \times 4.0$  m<sup>2</sup> (PC6);
- iii) muon filtering, behind the beam dump, is provided by the electron calorimeter (12 cm of lead), by the hadron calorimeter (1 m of iron) and by an additional iron absorber 80 cm thick;
- iv) the trigger system consists of two symmetric telescopes of counters and chambers placed above and below the horizontal plane.

A "pretrigger" is provided by three planes of counter hodoscopes:

- T<sub>1</sub> placed at the end face of the beam dump consisting of 12 counters;
- T<sub>2</sub> which is in fact the second layer of the electron calorimeter, subdivided in 50 horizontal strips;
- T<sub>3</sub> is the last hodoscope made of 44 horizontal sheets.

The last two hodoscopes cover vertical angles from  $\pm 6$  mrad up to  $\pm 165$  mrad. The pretrigger requires at least 2 particles in the coincidence T<sub>2</sub>T<sub>3</sub> and at least one in T<sub>1</sub>. The pretrigger provides a fast strobe for the proportional chambers PC1, PC2, M1 and M2.

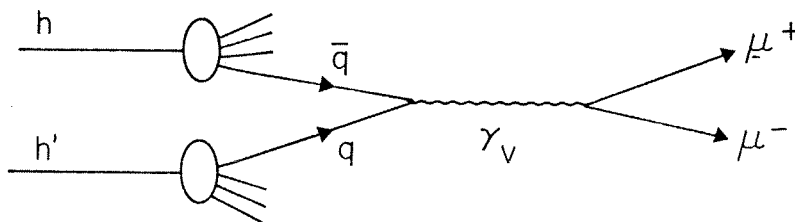
The trigger acts on the vertical component  $p_t^V$  of the transverse momentum of the muons. The  $p_t^V$  selection is achieved by two planes of cathode-readout chambers M1 and M2 covering vertical angles from  $\pm 30$  mrad up to  $\pm 165$  mrad. The cathodes are printed in 18 separated horizontal bands, each subdivided into 64 cells corresponding to equal intervals of the tangent of the azimuthal angle. The correlation between cells of a given band provides a cut-off in the magnetic deflection angle and thus in  $p_t^V$ , which in turn, defines a rough lower cut in the muon pair effective mass. The trigger conditions in the course of the experiment were either  $p_t^V > 0.7$  GeV/c for both muons,

or  $p_t^V > 1 \text{ GeV}/c$  for one muon, without cut on the other muon. Events with both muons in the 30 mrad cone of the W/U core of the beam dump were not accepted. The trigger system is illustrated in fig. 1(b).

The overall acceptance of the apparatus, as determined by the geometry of the detector and by the  $p_t^V$  cut is shown in fig. 1(c) as a function of the dimuon mass and of the variable  $x = 2p_L^*/\sqrt{s}$ , where  $p_L^*$  is the longitudinal momentum of the dimuon in the c.m. system.

### 3. DATA ANALYSIS

We analyse our data in the framework of the Drell-Yan mechanism, assuming that an antiquark  $\bar{q}$  and a quark  $q$  of the beam and target hadrons annihilate electromagnetically into a virtual photon which then decays into a muon pair, according to the diagram



The muon pair momentum and invariant mass  $M$  determine the kinematical variables of the colliding  $\bar{q}q$  pair, if transverse momentum is neglected, as

$$M^2 = x_1 x_2 s, \quad x = x_1 - x_2$$

where  $x_1$  and  $x_2$  are the fractional momenta of the quarks in the beam and target particle respectively.

The Drell-Yan formula can be written as

$$\frac{d^2\sigma}{dx_1 dx_2} = \frac{\sigma_0}{3} \sum_i \frac{Q_i^2}{x_1^2 x_2^2} \left[ f_i(x_1) f_{\bar{i}}(x_2) + f_{\bar{i}}(x_1) f_i(x_2) \right], \quad (1)$$

where  $\sigma_0 = 4\pi\alpha^2(\hbar c)^2/3s$  and the structure function  $f_i$  for quarks of flavour  $i$  and charge  $Q_i$  have a valence and a sea contributions,  $f_i = f_{iV} + f_{iS}$ . The factor of 3 due to the colour hypothesis is displayed explicitly in eq. (1).

For the pion there is a single valence function, that we call  $V(x_1)$ , defined by:

$$V(x_1) = \bar{u}_V^{\pi^-}(x_1) = d_V^{\pi^-}(x_1) = u_V^{\pi^+}(x_1) = \bar{d}_V^{\pi^+}(x_1).$$

For the nucleon there are two independent valence functions, that we define for the proton as  $u(x_2)$  and  $d(x_2)$  for the up and down quarks respectively:

$$u^p(x_2) = d^n(x_2) = u(x_2), \quad d^p(x_2) = u^n(x_2) = d(x_2).$$

The valence structure functions are normalized to the corresponding number of valence quarks i.e.

$$\int \frac{V(x_1)}{x_1} dx_1 = 1, \quad \int \frac{u(x_2)}{x_2} dx_2 = 2, \quad \int \frac{d(x_2)}{x_2} dx_2 = 1.$$

The sea distributions are taken to be SU3 symmetric. For each flavour, we define  $S_n(x_2)$  for the nucleon and  $S_\pi(x_1)$  for the pion.

In the analysis of our results we compare the experimentally determined cross section to the one calculated by the Drell-Yan formula using:

$$\left( \frac{d^2\sigma}{dx_1 dx_2} \right)_{\text{exp}} = K \left( \frac{d^2\sigma}{dx_1 dx_2} \right)_{\text{D.Y.}}, \quad (2)$$

where  $K$  is a scale factor, related either to our experimental normalization error or to a multiplicative correction factor due to QCD effects<sup>2)</sup>.

The general form of the cross section for pion-nucleon interaction is,

$$\frac{d^2\sigma}{dx_1 dx_2} = \frac{K\sigma_0}{3x_1^2 x_2^2} \left[ V(x_1) G(x_2) + S_\pi(x_1) H(x_2) \right], \quad (3)$$

where, for Pt target ( $Z/A = 0.40$ ), the nucleon functions  $G(x_2)$  and  $H(x_2)$  take the following form,

$$\begin{aligned} G &= 1/9 (1.6u + 2.4d + 5S_n) \quad \text{for } \pi^- \\ G &= 1/9 (0.6u + 0.4d + 5S_n) \quad \text{for } \pi^+ \\ H &= 1/9 (2.2u + 2.8d + 12S_n) \quad \text{for } \pi^\pm. \end{aligned} \quad (4)$$

The raw data of the experiment come in the form of  $\mu^+ \mu^-$  events for which we know the mass and the longitudinal momentum. From these we extract values of  $x_1$  and  $x_2$  for each event and we obtain an array as shown in fig. 2.

We have calculated by Monte Carlo method the acceptance at each value of  $x_1$  and  $x_2$ , by integrating on the observed  $p_t$  distribution and on the  $\cos\theta$  and  $\phi$  distribution<sup>1)</sup> which was taken to be  $P(\theta, \phi) \propto (1 + \cos^2\theta)$ . The experimental errors ( $\Delta p/p$ , multiple scattering) and the Fermi motion of the nuclear target distort slightly the distribution of events in the  $x_1, x_2$  array. The main effects are that the  $\Delta p/p$  error produces a  $\Delta x_1/x_1$  of about 3% at high  $x_1$ , while Fermi motion and multiple scattering induces  $\Delta x_2/x_2$  of about 10% and 6% respectively. The resulting effects on  $dN/dx_1$  are sizeable only at high  $x_1$  or  $x_2$  and in any case do not exceed 10%.

From the  $x_1, x_2$  array, corrected for acceptance, we extract the pion and nucleon structure functions by three different methods illustrated in the following sect. 3.1, 3.2, 3.3.

We exclude the mass regions where resonances are present, by the following cuts,  $4 < M < 8.5$  GeV/c<sup>2</sup> at 200 GeV/c and  $4.5 < M < 8.5$  GeV/c<sup>2</sup> at 280 GeV/c. In the resulting arrays we have 5607 events for 200 GeV/c  $\pi^-$ , 2073 events for 200 GeV/c  $\pi^+$  and 3441 events for 280 GeV/c  $\pi^-$ .

### 3.1 Factorization method

In this method we perform a first analysis of our  $\pi^-$  data by assuming that for the range of  $x_1$  values explored by this experiment, the sea of the pion can be neglected in comparison to the valence. In that case the observed cross section for incident  $\pi^-$  can be written as (see eq. 3)

$$\frac{d^2\sigma}{dx_1 dx_2} \propto \frac{1}{x_1^2 x_2^2} V(x_1) G(x_2).$$

For each bin of given  $x_1$  ( $N_1$  bins in total) we have an unknown value of  $V(x_1)$ , for each bin of given  $x_2$  ( $N_2$  bins in total) we have an unknown value of  $G(x_2)$ . We thus have  $N_1 + N_2$  unknown and  $N_1 \cdot N_2$  independent cells. We exclude from the analysis the cells where the acceptance is less than 3%. By minimizing the global  $\chi^2$ , we obtain the numerical value of the function  $V(x_1)$  for  $N_1$  different values of  $x_1$  and the numerical value of  $G(x_2)$  for  $N_2$  values of  $x_2$ .

The results of this analysis are shown for the 200 GeV  $\pi^-$  run in fig. 3(a) together with results from a similar analysis by Newman et al.<sup>3)</sup> on their 225 GeV  $\pi^-$  data. The  $\chi^2$  of our fit is 95 for 67 degrees of freedom. This value of the  $\chi^2$  indicates that in our kinematical range of the variable  $x_1$  and  $x_2$ , the factorization hypothesis may not be adequate.

We can also perform a simultaneous analysis of our  $\pi^-$  and  $\pi^+$  data without any assumptions on the pion sea. In fact the subtraction of the  $\pi^+$  induced

Drell-Yan cross section from the  $\pi^-$  induced cross section, allows to eliminate the terms involving the sea of the pion and those involving the sea of the nucleon, which are the same for incident  $\pi^+$  and  $\pi^-$ . For the Pt target ( $Z/A = 0.40$ ), the combination of up and down valence quark that we obtain is  $u + 2d$

$$\left( \frac{d^2\sigma}{dx_1 dx_2} \right)_{(\pi^- \text{Pt})} - (\pi^+ \text{Pt}) \propto \frac{1}{x_1^2 x_2^2} V(x_1) \frac{1}{9} [u(x_2) + 2d(x_2)].$$

The analysis was done by subtracting in each  $x_1, x_2$  cell the  $\pi^+$  events from the  $\pi^-$  events, both normalized to the same number of incident pions. This normalization was obtained by using the observed number of  $J/\psi$  events and the measured equality (within  $\pm 2\%$ ) of the production cross section for  $J/\psi$  on Pt by incident  $\pi^+$  and  $\pi^-$ ). The results are presented in fig. 3(b). The  $\chi^2$  of this  $\pi^- - \pi^+$  difference fit is 43 for 59 degrees of freedom. In the present analysis by the factorization method we have made no attempt of normalization of our data.

### 3.2 Parametrization method

We assume the following simple x-dependence for the various structure functions<sup>5)</sup>:

$$\begin{aligned} V(x) &= Ax^\alpha(1-x)^\beta \\ S_\pi(x) &= B(1-x)^n \\ u(x) &= A'_u x^{\alpha'}(1-x)^{\beta'} \\ d(x) &= A'_d x^{\alpha'}(1-x)^{\beta'+1} \\ S_n(x) &= B'(1-x)^{n'}. \end{aligned}$$

The choice of  $\alpha'_u = \alpha'_d$  and  $\beta'_d = \beta'_u + 1$  is the result of theoretical prejudices.

As explained in sect. 3, the parameter  $A, A'_u, A'_d$  are fixed in terms of  $\alpha$  and  $\beta$  by the normalization condition to the number of valence quarks.

If we use simultaneously the information from our  $\pi^-$  and  $\pi^+$  data, it is possible to determine the parameters of the sea in addition to the valence. In fact the  $\pi^+/\pi^-$  ratio gives the relative importance of the sea and the valence contribution, the variation of this ratio as a function of  $x_1$  and  $x_2$  fixes the relative importance of the pion sea and the nucleon sea.

The results of this global fit, done by a maximum likelihood method, on the 200 GeV data are given below:

$$\begin{array}{ll}
 \alpha = 0.40 \pm 0.06 & \alpha' = 1.02 \pm 0.15 \\
 \beta = 0.90 \pm 0.06 & \beta' = 4.04 \pm 0.4 \\
 B = 0.09 \pm 0.06 & B' = 0.35 \pm 0.07 \\
 n = 4.4 \pm 1.9 & n' = 6.0 \pm 1.3 \\
 A = 0.55 & A'_u = 10.5 \qquad A'_d = 6.31 .
 \end{array}$$

Only the relative normalization of the  $\pi^+$  to the  $\pi^-$  data (known within  $\pm 2\%$ ) is used in this fitting procedure. The absolute normalization, which is however affected by a large error, will be exploited in the following method to evaluate the factor K as defined by eq. (2).

### 3.3 Projection method

By projecting the content of the  $x_1, x_2$  array on the two axes we get the distribution  $dN/dx_1$  and  $dN/dx_2$ . If L is the integrated luminosity calculated from the integrated beam intensity and from the useful number of target nucleons assuming a linear A dependence<sup>1)</sup> of the cross section, we can get from eq. (3) and (4) an expression where only the variable  $x_1$  appears

$$F_{\pi}(x_1) \equiv \frac{dN/dx_1}{\frac{\sigma_0}{3} \frac{L}{x_1^2} I(x_1)} = K \left[ V(x_1) + \frac{J(x_1)}{I(x_1)} S_{\pi}(x_1) \right]. \quad (5)$$

In this equation the quantities  $I(x_1)$  and  $J(x_1)$  are integrals involving the nucleon structure functions  $G(x_2)$  and  $H(x_2)$  and the calculated acceptance of the apparatus  $A(x_1, x_2)$

$$I(x_1) = \int \frac{G(x_2)}{x_2^2} A(x_1, x_2) dx_2, \quad J(x_1) = \int \frac{H(x_2)}{x_2^2} A(x_1, x_2) dx_2.$$

These integrals have been evaluated in two different ways:

- i) using the results of the fit to our data discussed in sect. 3.2;
- ii) using the results of the CDHS<sup>6)</sup> parametrization.

The quantity  $J(x_1)/I(x_1)$  is nearly constant ( $\pm 7\%$ ) in the relevant  $x_1$  range and is  $\sim 1.4$  for the  $\pi^-$  data and  $\sim 3.7$  for the  $\pi^+$  data. In fig. 4(a) we present the results for the pion structure function.

A procedure similar to the one which leads to eq. (5) can be used to derive the nucleon structure function using as input the pion structure function from our fit. In this case for the  $\pi^-$  the valence part is  $1.6u + 2.4d$  and  $J/I \sim 5.3$ , for the  $\pi^+$  the valence part is  $0.6u + 0.4d$  and  $J/I \sim 4.5$ . The results are given in fig. 4(b).

The numerical value of  $K$  is obtained from the integration of eq. (5)

$$K = \frac{\int F_{\pi}(x_1) dx_1}{\int \left[ V(x_1) + \frac{J(x_1)}{I(x_1)} S_{\pi}(x_1) \right] dx_1},$$

where  $V(x_1)$  and  $S_{\pi}(x_1)$  are the normalized valence and sea structure functions as determined in sect. 3.2. The results on  $K$  are given in table 1.

#### 4. DISCUSSION

a) First we should note that the shape of the pion structure function is rather insensitive to the choice of the nucleon structure function used in the projection method of sect. 3.3. Furthermore, the pion and nucleon valence structure function curves obtained from our fit fall nicely on the values obtained from the factorization method (sect. 3.1) using the  $\pi^- - \pi^+$  data (fig. 3(b)); this checks the consistency of the two methods. The  $\pi^-$  structure function which we derive from the factorization method agrees in shape with the result of Newman et al.<sup>3)</sup>. However, the nucleon structure functions, derived by the same methods, are incompatible (fig. 3(a)).

b) Using the parameters obtained from our fit in sect. 3.2, we find:

$$2 \cdot \int V(x_1) dx_1 = 0.34 \quad 6 \cdot \int S_{\pi}(x_1) dx_1 = 0.10 .$$

These fractions of the  $\pi$  momentum carried respectively by the valence quark and the sea agree with general expectation.

On the other hand, using the parameters from the same fit, we find:

$$\int (u(x_2) + d(x_2)) dx_2 = 0.47 \quad 6 \cdot \int S_N(x_2) dx_2 = 0.3 .$$

Our nucleon structure functions (and their integrals) are about twice as high as those obtained in the parametrization of CDHS. It should be noticed however that in our fit we are very sensitive to extrapolation of the structure function to  $x_2 = 0$  and hence the values given above, both for the sea and valence, depend on the choice of the analytical representation of  $F_N(x_2)$  at small  $x_2$ <sup>7)</sup>. It should also be noticed that a large value of the nucleon sea momentum, compatible with ours, is obtained in the analysis of the FNAL proton data<sup>8,9)</sup>.

c) The values of the scale factor  $K$  given in table 1 are affected by different sources or errors; they are listed in table 2.



REFERENCES

- 1) J. Badier et al., "Muon pair production above 4 GeV (Drell-Yan continuum) by  $\pi^\pm$ ,  $K^\pm$ ,  $\bar{p}$  and  $p$  at 200 GeV/c and by  $\pi^-$  at 280 GeV/c on platinum and hydrogen targets", International Conference on High Energy Physics, Geneva 1979.
- 2) G. Altarelli et al., MIT Report CTP No 776, 1979.  
J. Kubar-André and F.E. Paige, Phys. Rev. D19 (1979) 221.
- 3) C.B. Newman et al., Phys. Rev. Lett. 42 (1979) 951.
- 4) J. Badier et al., "Dimuon resonance production from 200 and 280 GeV/c tagged hadron beam", International Conference on High Energy Physics, Geneva 1979.
- 5) A.J. Buras and K.J.F. Gaemers, Nucl. Phys. B132 (1978) 249.
- 6) J.G.H. de Groot et al., Phys. Lett. 82B (1979) 456.
- 7) The larger acceptance error in the case of the fit with our data alone is due to the strong dependence of the integral  $\int F_N(x_2)/x_2 dx_2$  on the acceptance at small  $x_2$ .
- 8) L.M. Lederman, Proc. of the 19th International Conference on High Energy Physics, Tokyo, 1978.
- 9) E.L. Berger, SLAC-PUB-2314, 1979.

Table 1

Results on the scale factor K

	$\pi^+$ 200 GeV/c	$\pi^-$ 200 GeV/c	$\pi^-$ 280 GeV/c
G(x <sub>2</sub> ), H(x <sub>2</sub> ) from this experiment (sect. 3.2)	1.4	1.4	1.5
G(x <sub>2</sub> ), H(x <sub>2</sub> ) from CDHS fit	2.4	2.2	2.5

Table 2

Estimated errors on the scale factor K

	K obtained using for the nucleon G(x <sub>2</sub> ) and H(x <sub>2</sub> ) from CDHS	K obtained using for the nucleon G(x <sub>2</sub> ) and H(x <sub>2</sub> ) from our fit
Luminosity error of our experiment	± 15%	± 15%
statistical error	± 10%	± 15%
Systematic error from the acceptance uncertainty	± 10%	± 15%
CDHS normalisation error	± 5%	-

FIGURE CAPTIONS

- Fig. 1(a) General layout of the NA3 spectrometer for the study of dimuon production in hadronic collision.
- (b) Sketch of the trigger system.
- (c) The acceptance of the apparatus as a function of  $x$  and  $M$  as calculated by a Monte-Carlo method.
- Fig. 2 Two-dimensional plot in the  $x_1, x_2$  plane of the 200 GeV/c  $\pi^-$  Pt dimuon events. A cut was applied at  $M = 4 \text{ GeV}/c^2$ .
- Fig. 3(a) The data points are the result of the factorization method (sect. 3.1) applied on the  $\pi^-$  data at 200 GeV/c. Data points from ref. 3) are also plotted with arbitrary relative normalization. The shape of the structure functions obtained by the parametrization method (sect. 3.2) is also shown.
- (b) The data points are the result of the factorization method (sect. 3.1) applied to the  $\pi^- - \pi^+$  data at 200 GeV/c. The shape of the structure functions obtained by the parametrization method (sect. 3.2) is also shown.
- Fig. 4(a) The data points represent  $F_{\pi}(x_1)$  as defined by eq. (5), using:
- nucleon structure function  $\pi$  of our fit (1)
  - nucleon structure function from CDHS fit (2)
  - i) dashed curves represent the valence structure function of the pion obtained from our fit.
  - ii) solid curves represent the (valence + sea) pion structure function as defined by eq. (5).
- The curves have been scaled up by a factor  $K$ :  
( $K = 1.4$  for (1),  $K = 2.5$  for (2))
- (b) The data points represent  $F_N(x_2)$ , as defined in sect. 3.3, using the pion structure function  $N$  from our fit.
- dashed curves represent the valence part of the nucleon structure function:  $1.6u(x_2) + 2.4d(x_2)$  for  $\pi^-$   
 $0.4d(x_2) + 0.6u(x_2)$  for  $\pi^+$
  - solid curves represent (valence + sea) nucleon structure function as defined in sect. 3.3.
- The curves have been scaled up by a factor  $K$ :  
( $K = 1.4$  using our fit;  $K = 2.5$  using CDHS fit).

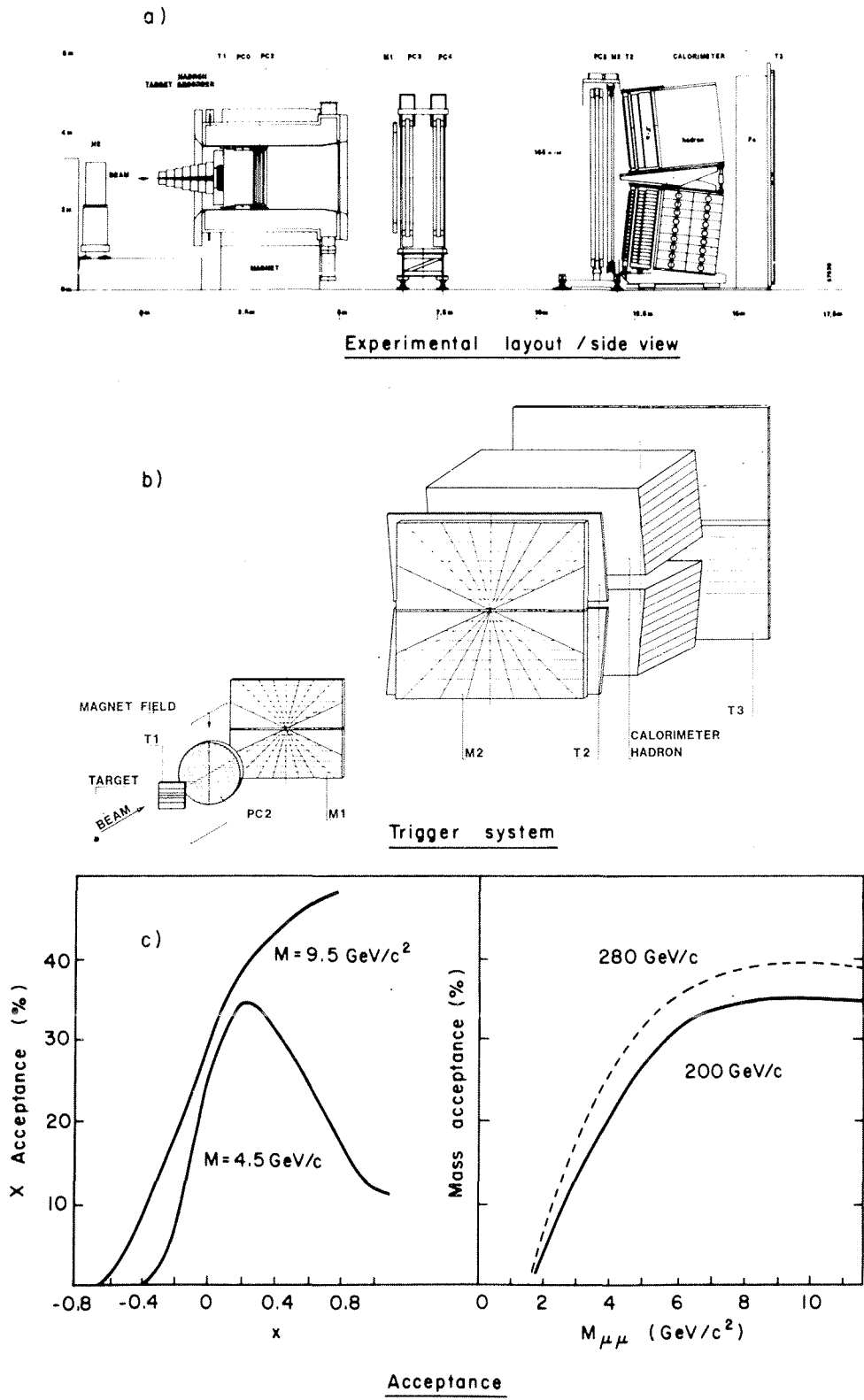


Fig. 1

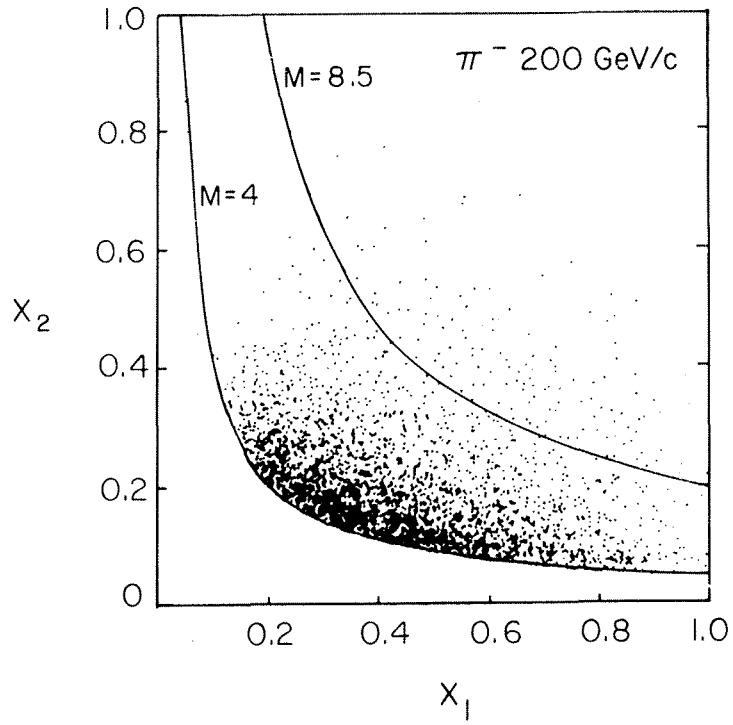


Fig. 2

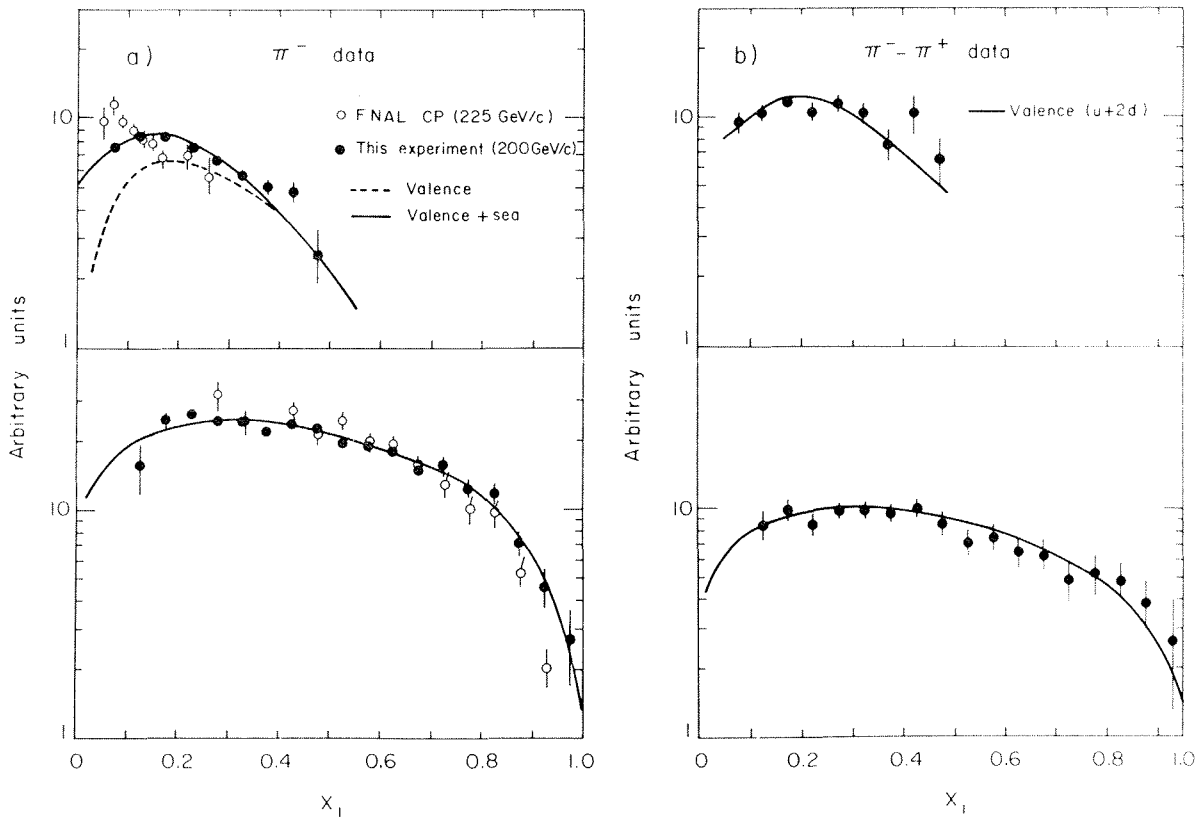


Fig. 3

PION

NUCLEON

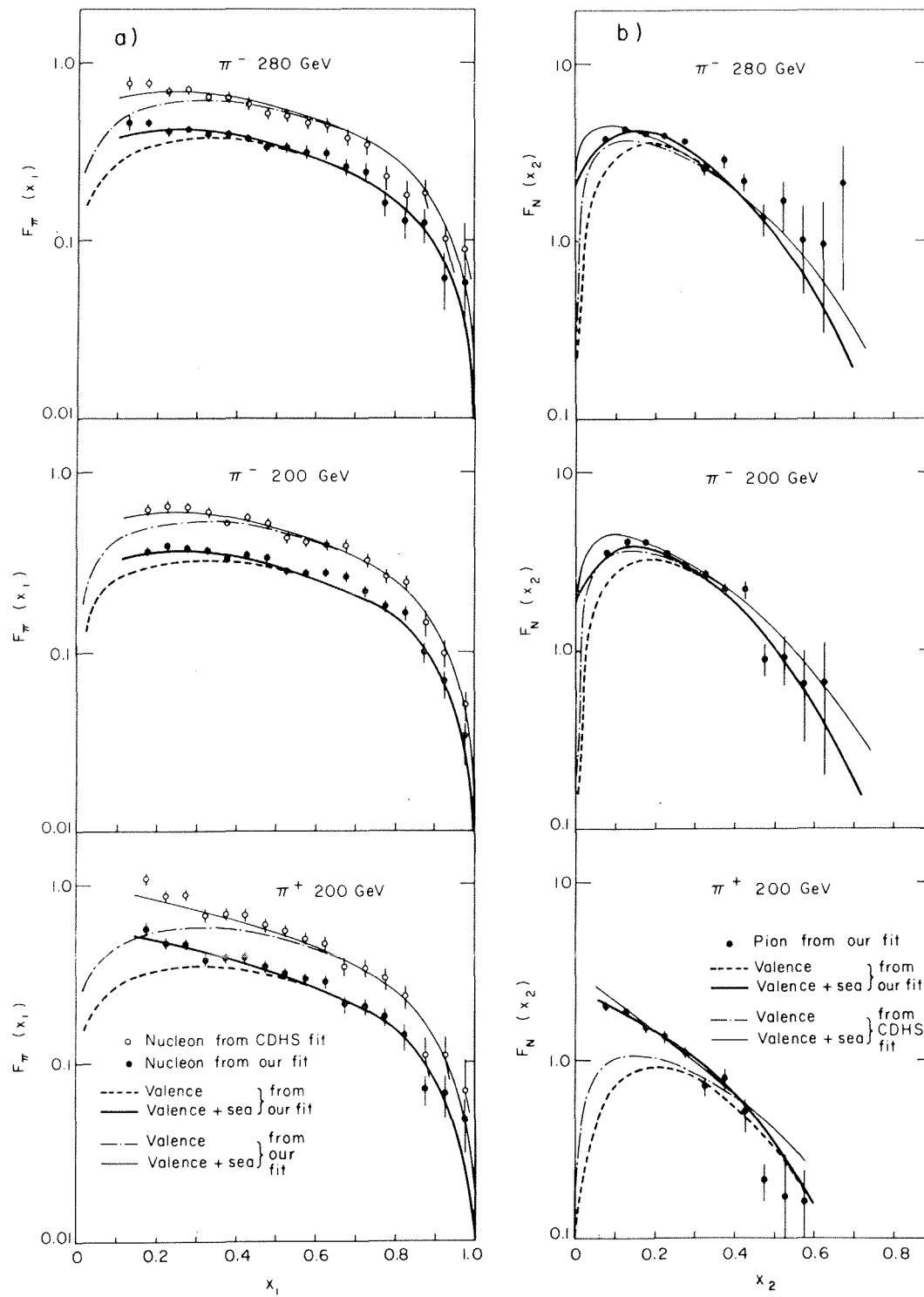


Fig. 4